Hindawi
Geofluids
Volume 2022, Article ID 7290894, 14 pages
https://doi.org/10.1155/2022/7290894

Research Article

Study on Reasonable Chain Pillar Size in a Thick Coal Seam

Kun Zhang,[1,2] Fengfeng Wu,[1,2] and Xin Yue[1,2]

[1]*Key Laboratory of Deep Coal Resource Mining, Ministry of Education, China University of Mining and Technology, Xuzhou 221116, China*
[2]*School of Mines, China University of Mining and Technology, Xuzhou 221116, China*

Correspondence should be addressed to Fengfeng Wu; wufengfeng@cumt.edu.cn

Received 24 September 2021; Revised 12 December 2021; Accepted 8 February 2022; Published 23 March 2022

Academic Editor: Mohammed Fattah

In order to solve the problem of low coal recovery rate caused by leaving large coal pillars in deep mines, the study determined the reasonable width of the section pillar, which based on the theory of coal pillar stress distribution, taking the 4102 headgate of Wenjiapo coal mine as the engineering background. Field monitoring and numerical simulation results show that the influence range of the lateral abutment pressure in the goaf is 50~56 m, and the abutment stress distribution in the coal pillar resembles a hump with two peaks of 38.9 MPa and 33.6 MPa, respectively. The positions of the double peaks are located at 12 m and 36 m in the coal pillar, respectively. In the range of "hump," the section pillar vertical stress is in the original rock stress and is relatively stable. It can be regarded as an elastic zone in the coal pillar with strong bearing capacity, the coal in other areas have already undergone plastic yielding, and the bearing capacity has been reduced; the width of coal pillars in the determined section has been reduced from 46 m to 33 m, which is a reduction of 13 m. The research results have been applied in the 4106 headgate in the same mining area, and good test results have been obtained. The maximum subsidence of the roof-to-floor and rib-to-rib convergence is 286 mm and 150 mm, this indicates that its deformation was within the allowable limits, and the cross-section area was sufficient to satisfy the requirements.

1. Introduction

More than 90% of underground mines use longwall mining methods, and coal pillar has always been the main way to isolate the goaf and maintain the roadway in Chinese coal mine mining [1]. According to the current research status at home and abroad, there are mainly two ways to retain coal pillar. The first is the wide coal pillar method, which arranges the roadway outside the pressure peak to reduce the damage to the roadway; the other is the yield pillar or nonpillar method, which is used to reduces the width of coal pillar and reduces resource waste [2–4].

The research and development level of the two roadway protection methods also have their own characteristics, and they have been widely used under different conditions. Coal mines in central and western China (Shanxi, Shaanxi, Inner Mongolia, etc.) have gradually entered the stage of deep thick seam mining [5]. However, the actual production process of most existing coal mines has been troubled by the width of coal pillars, which are mostly 50 m in width. Above, large coal pillars not only cannot be recovered but also easily cause the roadway to be arranged in the stress-increasing area, which is an important reason of major accidents [6–8]. Especially now scientific and green mining is advocated, higher requirements are put forward for the determination of the width of coal pillars.

In terms of theoretical research, domestic and foreign scholars have done a lot of research on coal pillar retention and put forward various theories such as effective area theory, large slab fissure theory, two-zone constraint theory, and limit equilibrium theory [9–12]. Each theory has certain applicable conditions: the effective area theory can only be used when the excavation area is large, the width and interval of the coal pillars are the same, the width of the plastic zone calculated by the large slab crack theory is proportional to the width of the coal pillar, obviously inconsistent with the actual situation, and the two-zone constraint theory believes that the coal pillar is composed of a yield zone and an elastic core zone, which better explains the form of the stress distribution of the coal

pillar, but the selection of the relevant parameters of the formula requires a large amount of on-site measured data or coal and rock strength test.

Domestic research on the distribution of abutment pressure in the coal pillar is mostly based on the theory of limit equilibrium zones. The most important thing for the establishment of related models and theoretical derivation is to establish a reasonable basis for determining the limit equilibrium state [13–16]. Hou et al. deduced the corresponding abutment pressure distribution formula and gave the calculation method of the width of the limit equilibrium zone and applied it in the coal pillar setting of the mining area [17]. Kang et al. explained the setting of coal pillars under different circumstances, such as nonpillar and yield pillar [18–20]. Based on the analysis of the overlying rock movement characteristics of the stope, Zhang et al. clarified the transfer load-bearing mechanism of the roof in the wedge-shaped area on the goaf side and proposed the technical idea of optimizing the residual stress of the coal pillar [21]. Li et al. analyzed the deformation of the roadway surrounding rock under different coal mine geological conditions and found that the factors affecting the stability of yield coal pillar include: coal seam strength, coal seam thickness, coal seam depth, immediate roof strength, influence of driving and mining, support strength, and narrow coal pillar width [22].

Combined with field tests and numerical simulation, the width of section pillar is proved to be reasonable is also studied. The influence law of the reasonable width of the coal pillar is studied, and on this basis, a method that can not only meet the stability requirements of the coal pillar but also improve the resource recovery rate is proposed. The research results will provide a theoretical basis for the economy and safety of section pillar.

2. Background

2.1. Engineering Background. Wenjiapo Mine located in the Binchang coal mining area was a typical Chinese deep coal mine, with an excavation depth of almost 600 m ~700 m below the ground. The shaft station was buried at an average burial depth of 650 m. The entry was a rectangular section with a width of 5.7 m and a height of 3.65 m. The fully mechanized full seam top coal caving mining method was employed. The width of the section pillar is 46 m (see Figure 1), the coal pillar is relatively broken during the mining, and stability of the surrounding rocks of the roadway is bad. The width of the coal pillar needs to be optimized.

The 4102 headgate is in the 4# coal seam, with an average thickness of 4.8 m. The roof rock strata are, in ascending order, mudstone (2.31 m), fine sandstone (1.4 m), mudstone (2.1 m), powder sandstone (8.8 m), and coarse sandstone (10.2 m), while those below are, in descending order, mudstone (2.6 m), medium sandstone (6.7 m), and siltstone (9.1 m). The roadway has a height of 3.65 m and a width of 5.7 m (Figure 2).

2.2. Determination of Rock Mechanic Parameters. In order to have a detailed understanding of the surrounding rock properties of 4102 headgate, the surrounding rock of 4102 headgate was selected to collect coal and rock samples without structural belts and faults, avoiding the construction of the project, and after the sampling was completed, the PVC was sealed in the underground, after being transported to the laboratory for standardized processing (see Figure 3).

The rock mechanics parameters are measured on the SANS (TAW-2000) microcomputer controlled electrohydraulic servo rock triaxial testing machine (see Figure 4). The maximum axial load of the test system is 2000 kN, the maximum lateral pressure is 500 kN, and the maximum shear load is 500 kN.

After sampling in the 4102 headgate, standard specimens were made, and the rock mechanics performance parameters were measured as shown in Table 1.

3. Theoretical Analysis Stress Distribution in the Coal Pillar

After the roadway excavation is finished, the overburden pressure is redistributed, and a certain range of mining-induced stress zone will be formed in the coal pillar. Due to the influence of the mining-induced stress, it is believed that the coal and rock mass within a certain width of the coal pillar has been damaged. It is generally believed that the abutment pressure at the edge of the coal pillar is zero. As the depth increases, the abutment pressure gradually increases until it reaches the peak value of the vertical stress in the coal pillar [23–25]. The specific area from the coal pillar boundary to the peak vertical stress is called the yield zone and is also called the plastic zone width in the coal pillar [26–28].

3.1. The Vertical Stress Distribution in the Coal Pillar after Working Face Mining. In this section, the coal pillar is divided into inner plastic zone and elastic zone, and the study is carried out according to the quadratic curve. The integrated coal vertical stress in the plastic zone is calculated by the theory of limit equilibrium zone, and the integrated coal stress in the elastic zone is fitted by the Weibull distribution function. Substituting the relevant parameters to obtain the vertical stress in the coal pillar and finally determine the reasonable width of the coal pillar. In theoretical calculations, some necessary assumptions should be made to make the answer to the problem simple. The basic assumptions are [29–31] as follows:

(1) The coal pillar is regarded as an ideal elastic body, which conforms to the reasonable assumptions of continuity, complete elasticity, uniformity, and isotropy in elastic mechanics

(2) The internal shear damage in the coal pillar obeys the Mohr Coulomb criterion

(3) The stress limit equilibrium zone is at the elastic-plastic junction

(4) Before the coal pillar yields, the internal displacement and deformation in the coal pillar are small

After the roadway excavation is finished, the vertical stress distribution in the integrated coal is plotted as curves (see Figure 5).

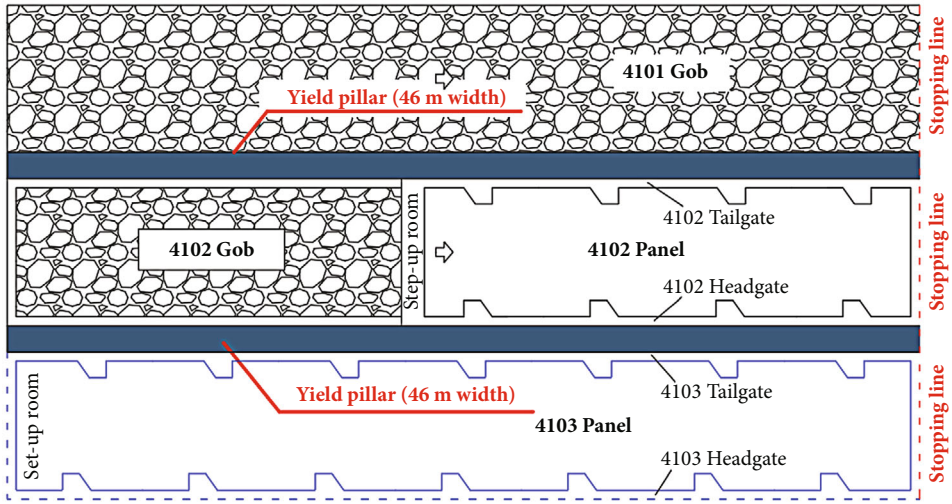

Figure 1: Schematic diagram of the project.

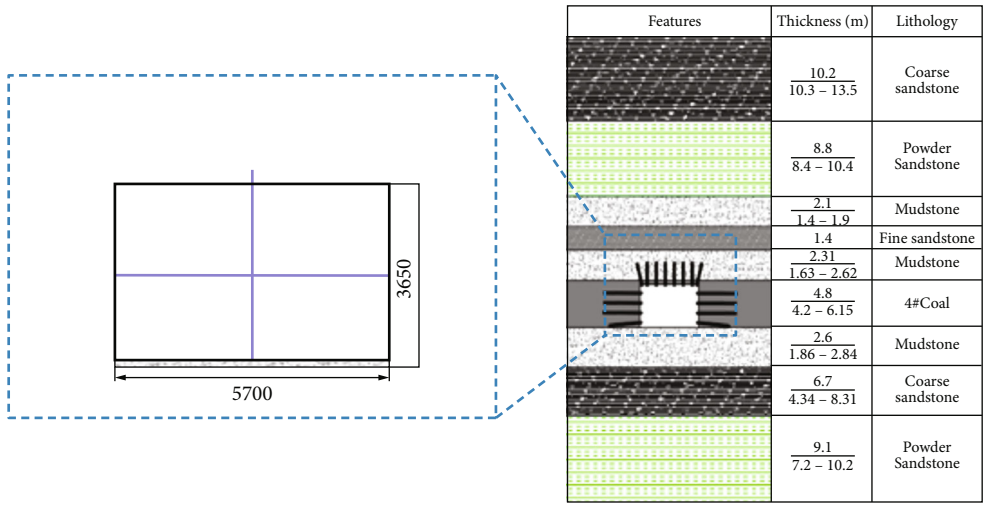

Figure 2: The lithological characteristics of the section and surrounding rock of 4102 headgate.

Figure 3: No. 4 coal seam rock formation specimens.

Figure 4: Experimental system for determining rock mechanical properties.

In Figure 5, $F(\varepsilon)$ is the influence of working face mining on the vertical stress of on the right side of integrated coal, and $f_1(\varepsilon)$ is the influence on the integrated coal stress in the plastic zone. The vertical stress in the plastic zone of coal pillar (lateral abutment pressure) is the limit equilibrium state; $f_2(\varepsilon)$ is the influence on the stress elastic zone of coal pillar [32–34].

Table 1: Measurement results of rock mechanical parameters.

Lithology	Compressive strength/ MPa	Shear strength/ MPa	Tensile strength/ MPa	Poisson ratio	Cohesion/ MPa	Friction/°
Silty mudstone	11.3	29	1.8	0.29	6.8	35
Fine sandstone	50.9	86.7	2.8	0.24	13.2	49
Pelitic siltstone	30.4	50.4	2.2	0.28	11.1	36
Coal	5.8	9.1	1.4	0.32	3.4	29
Mudstone	9.7	21.1	1.59	0.3	5.3	32
Medium fine sandstone	46.4	39.5	2.7	0.26	11.7	46

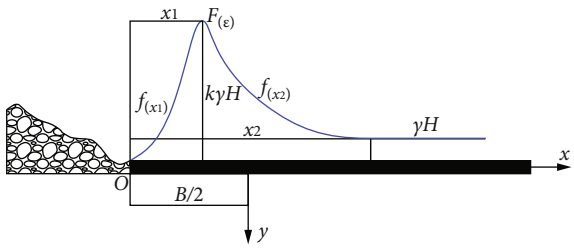

Figure 5: Vertical stress distribution in the integrated coal after working face mining.

It can be calculated by formula (1).

$$f_1(\varepsilon) = \left(\frac{C_0}{\tan\varphi} + \frac{p_i}{\lambda_1}\right) e^{\frac{2\tan}{m\lambda_1}(\varepsilon + B/2)} - \frac{C_0}{\tan\varphi} \varepsilon \in [-B/2,\ x_1 - B/2), \tag{1}$$

where C_0 is the coal seam interface cohesion, 6.62 MPa, φ is the internal friction angle of the coal seam interface, 28.81°, p_i is the bolt supporting strength, 0.2 MPa, λ_1 side pressure coefficient in the coal pillar, 1, m the height of the roadway, 3.8 m, B the width of coal pillar, 46 m, x_1 the plastic zone range in the coal pillar after working face mining, m.

The range of the plastic zone is calculated by formula (2):

$$x_1 = \frac{m\lambda_1}{2\tan\varphi} \ln\left[\left(k_1\gamma H + \frac{C_0}{\tan\varphi}\right) / \left(\frac{C_0}{\tan\varphi} + \frac{p_i}{\lambda_1}\right)\right], \tag{2}$$

where k_1 is the increasing coefficient vertical stress in coal pillar during working face mining.

The vertical stress in the coal pillar outside the plastic zone satisfies the Weibull distribution, and the Weibull distribution function expression is

$$w(x) = \mathrm{e}\frac{x}{x_w} e^{-\frac{x}{x_w}}, \tag{3}$$

where x is the random variable, the distance from any point of the original rock stress zone to the coal rib, and x_w is the scale parameter.

Combined with the distribution law of the internal stress of the coal pillar outside the plastic zone, substituting the relevant parameters, $f_2(\varepsilon)$ is

$$f_2(\varepsilon) = (k_1 - 1)\gamma H, \varepsilon \in [x_1 - B/2, +\infty), \tag{4}$$

where

$$s = \left(\varepsilon + x_f + B/2 - x_1\right)/x_{f_\circ}, \tag{5}$$

where γ is the bulk density, 2.5kN/m^3, H is the buried depth of the roadway, 650 m, and x_f is the parameter that adjusts the degree of urgency of the function.

In formula (4), $f_2(\varepsilon)$ is a single-peak function, and when $\varepsilon = x_1 - B/2$, the peak value $f_2(\varepsilon)$ is $k_1\gamma H$. The peak value $f_2(\varepsilon)$ increases with k_1; so, the value of the stress peak can be adjusted by changing it to reflect the degree of influence of the mining face on the peak abutment pressure of the coal pillar center. Increase or decrease x_f to adjust the degree of gradualness and urgency in the $f_2(\varepsilon)$ descending process during the $\varepsilon \longrightarrow +\infty$ process and gradually decrease to the original rock stress as it develops into the deep part of the coal seam. According to the above analysis, it can be seen that the influence of working face mining on the central abutment pressure in the coal pillar is

$$F(\varepsilon) = \begin{cases} \left(\frac{C_0}{\tan\varphi} + \frac{p_i}{\lambda_1}\right) e^{\frac{2\tan\varphi}{m\lambda_1}\left(\varepsilon + \frac{B}{2}\right)} - \frac{C_0}{\tan\varphi}, \varepsilon \in \left[-\frac{B}{2}, x_1 - \frac{B}{2}\right), \\ (k_1 - 1)\gamma H s e^{1-s} + \gamma H, \varepsilon \in \left[x_1 - \frac{B}{2}, +\infty\right). \end{cases} \tag{6}$$

3.2. Determination of the Reasonable Width of the Coal Pillar. According to the production geological conditions of Wenjiapo Mine and related test results, combined with numerical simulation results, the calculation parameters are as follows: average buried depth of roadway H is 650 m, rock layer density ρ is 2.5×10^3 kg/m^3, coal seam thickness h is 4.8 m, bolt supporting strength p_i is 0.2 MPa, coal seam cohesive force C_0 is 6.62 MPa, coal seam internal friction angle φ is 28.81°, integrated coal abutment pressure increases coefficient 1.5 after working face mining, the abutment pressure increase coefficient on one side of the body is 1.3, and the side pressure coefficient in the plastic zone is 1.0.

The basic condition for maintaining the stability of the coal pillar in the roadway protection is as follows: after plastic deformation occurs on both sides of the coal pillar, there is an elastic core with a certain width in the center of the coal

pillar, and the width of the elastic core is not less than twice the height of the coal pillar. Therefore, the reasonable width of coal pillar in the 4102 headgate face is

$$B > x_0 + 2h + x_1,$$
$$x_0 = \frac{h\lambda_1}{2\tan\varphi} \ln\left[\left(k_1\gamma H + \frac{C_0}{\tan\varphi}\right)/\left(\frac{C_0}{\tan\varphi} + \frac{P_i}{\lambda_1}\right)\right], \quad (7)$$

where x_0 is the width of plastic zone on the left side of the coal pillar, x_1 is the width of the plastic zone on the right side of the coal pillar, λ_1 is the increase coefficient of the abutment pressure in the integrated coal after the mining, 1.5, k_1 is the inner stress coefficient in the plastic zone is 1.0, and $\lambda 2$ is the increase coefficient of abutment pressure on the side of coal body after excavation of roadway 1.3.

$$x_1 = \frac{h\lambda_2}{2\tan\varphi} \ln\left[\left(k_1\gamma H + \frac{C_0}{\tan\varphi}\right)/\left(\frac{C_0}{\tan\varphi} + \frac{P_i}{\lambda_1}\right)\right]. \quad (8)$$

Because the width of the coal pillar is different, the width of the corresponding coal pillar's plastic zone is also different. Substituting the parameter to solve formula (8), x_0 is 11.2 m, x_1 is 8.9 m, and B is bigger than 29.7 m.

4. Measurement of Lateral Stress in Working Face

The borehole stress gauge was used to measure the stress distribution in the coal pillar during the 4102 working face mining in order to analyze the stress distribution of the coal pillar. Due to the large coal pillar width, it is difficult to construct horizontal small-diameter deep holes, and the drilling cannot penetrate the 46 m coal pillar. Therefore, the two roadways are arranged equally, and the measuring stations are arranged in front of the workface, that is, the 4102 headgate and the 4103 tailgate. The strain gauges are located 3 m, 6 m, 9 m, 12 m, 15 m, 18 m, and 21 m, within the pillar with a distance of about 1 m (see Figure 6).

After collecting and processing the measured data, the distribution of the abutment pressure in the coal pillar is obtain to draw a curve (see Figure 7).

The lateral abutment pressure in the coal pillar continues to increase with the mining (see Figure 7); the lateral abutment pressure distribution in the coal pillar resembles a hump with two peaks of 38.9 MPa and 33.6 MPa, respectively, and the positions of the double peaks are located 12 m and 36 m in the coal pillar, respectively. The range of the "hump" is roughly 17 m ~34 m. In the range of 17 m width range, the vertical stress in the coal pillar is 15 MPa~20 MPa, which is basically in the original rock stress with small difference. It can be regarded as an elastic zone with a certain width in the coal pillar and has a strong bearing capacity. The analysis shows that the width of the coal pillar can be appropriately reduced, and the width of the "hump" is can be reduced, but it still has enough elastic zone to play the bearing role.

It was suggested that the optimization of coal pillars can reduce the width of the "hump", and its width can be reduced from 46 m to 26~35 m.

5. Numerical Simulation Analysis of Coal Pillar Stress Distribution

Using the FLAC^{3D} software to simulate and analyze the stress distribution in the coal pillar and the deformation and failure process of the two mining roadways to provide guidance for the reasonable determination of the coal pillar width [35–37], the numerical model must meet the following conditions. In order to meet these conditions, the numerical model must have the following steps:

(1) Geometry and geology of the model, based in project information of mining and drilling

(2) Boundary conditions and restrictions on the edges of the model to simulate the continuity of the medium

(3) Material properties (solid rock) are found in the place, being these criteria-based properties of classification

(4) Initial stress field of the model, based on stress measurements or empirical methods

(5) Sequence of excavation of galleries to simulate the redistribution of stresses and displacements of the massif caused by the excavation

(6) Analysis of results to determine whether the rock mass or the type of treatment used for control of deformations is satisfactory (or not).

5.1. Numerical Model. Using FLAC^{3D} software to establish a numerical calculation model according to the geological conditions of Wenjiapo Mine, the model includes No. 4 coal and a total of 28 layers of upper and lower rock formations, and the size of the model is 206 × 150 × 91 m. Horizontal displacement constraints are imposed on the boundaries on both sides and front and rear boundaries, vertical displacement constraints are imposed on the bottom boundary, and uniformly distributed loads are imposed on the upper boundary. The uniformly distributed loads are calculated based on the weight of the overlying rock. The density of the overburden is 2500 kg/m^3, the buried depth of the No. 4 coal seam is determined to be 650 m, the uniform load of 16.95 MPa is applied to the upper part of the model to simulate the weight of the overburden, and the lateral pressure coefficient is 1.

The mechanical parameters of model coal and rock mass are shown in Table 2.

The numerical calculation model is balanced with the initial stress (see Figure 8).

5.2. Simulation of the Original Coal Pillar Width. The vertical stress distribution in the section coal pillars when the 4102 working face is advanced at 0 m, 40 m, 80 m, and 120 m is simulated and calculated the vertical stress distribution in the coal pillar (see Figure 9).

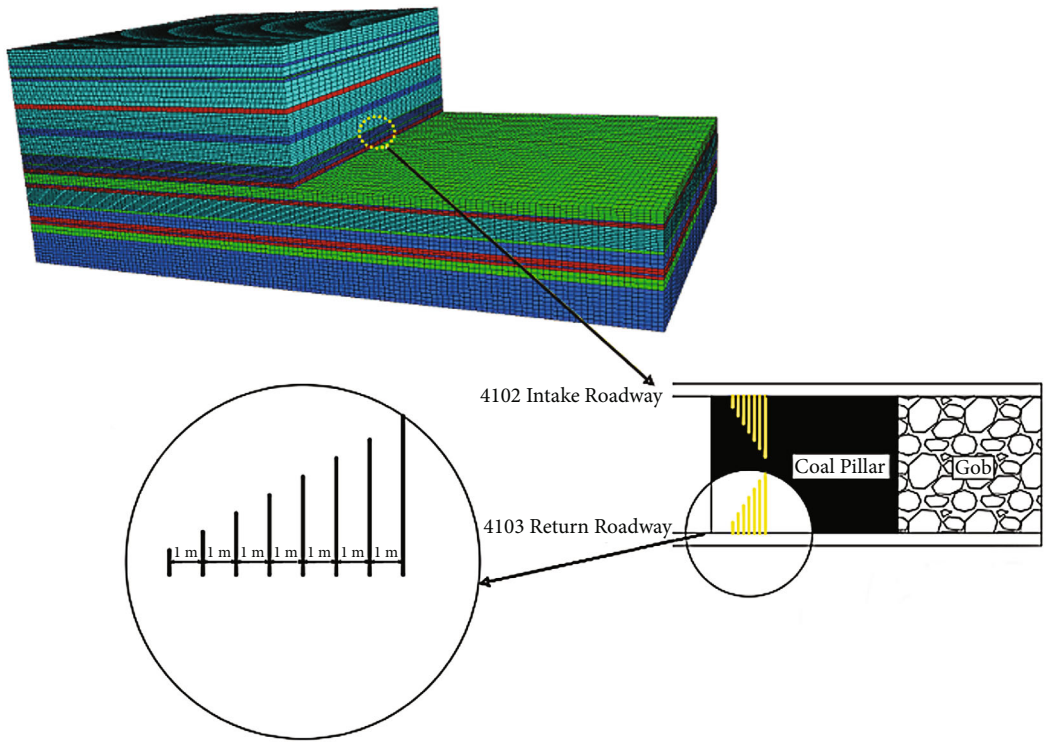

Figure 6: Borehole stress gauge monitoring station.

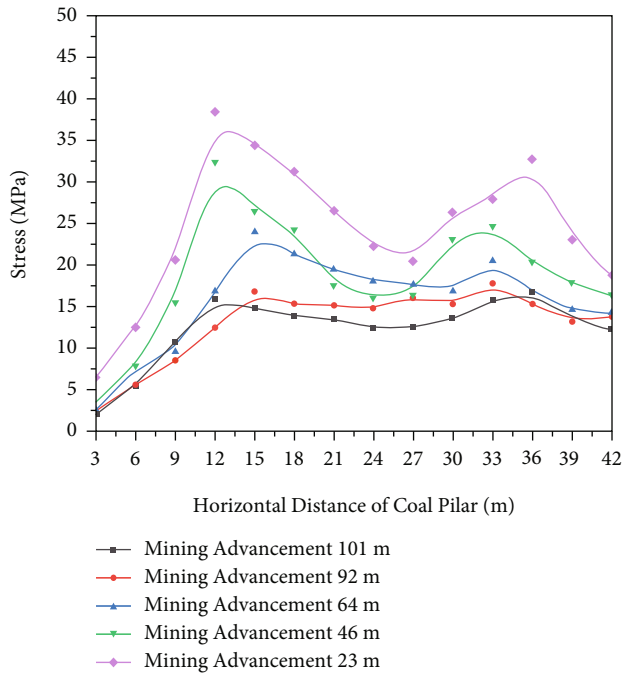

Figure 7: Distribution diagram of lateral abutment pressure in the coal pillar.

The vertical stress distribution data obtained by numerical simulation is plotted as curves (Figure 10).

It can be seen from Figure 10 that as the working face advancing, the vertical stress in the coal pillar continues to increase under the influence of mining-induced stress; the vertical stress distribution curve in the coal pillar resembles "a hump with two peaks" of 33.5 MPa and 34.3 MPa, respectively, the positions of the double peaks of each curve are approximately at 11 m and 37 m in the coal pillar, and the width of "hump" is roughly in the range of 17 m ~36 m. In the range of "hump," the abutment pressure in the coal pillar is 19 MPa~25 MPa, which is close to the stress of primary rock. It can be regarded as a certain width of elastic zone in the coal pillar, which has strong bearing capacity, and the coal in the other ranges has already undergone plastic yielding and only has a certain bearing capacity. The width of the "hump" (see Figure 10) can be appropriately reduced.

5.3. The Abutment Pressure Distribution Law in the Coal Pillar with Different Widths. According to the geological conditions of Wenjiapo Coal Mine, the coal pillar width x is 15 m, 25 m, 33 m, and 46 m, respectively and the abutment pressure distribution law in the coal pillar and the displacement of roadway surrounding rock during roadway driving and mining. The simulation process is divided into 4 steps: the first step is the calculation of the original rock stress balance; the second step is the calculation of the mining influence of the 4103 working face in the upper section; the third step is the roadway driving and bolt support of the 4102 working face in this section protection calculation; the fourth step is calculation of mining influence of 4102 working face in this section. The simulation diagram is shown (see Figure 11), where x is the width of the coal pillars, which are 15 m, 25 m, 33 m, and 46 m, respectively.

In the case of leaving coal pillars with different widths, the vertical stress in the coal pillars distribution was curve can be obtained directly by software (see Figure 12).

Table 2: Model parameters.

Lithology	Tensile strength/MPa	Cohesion/MPa	Friction/°	Bulk modulus/GPa	Shear modulus/GPa
Mudstone	1.25	1.70	26.44	0.82	0.49
Sandstone	1.51	1.47	23.16	0.70	0.46
Siltstone	1.43	3.14	35.85	1.07	0.77
Coal	0.72	1.99	26.81	0.35	0.14

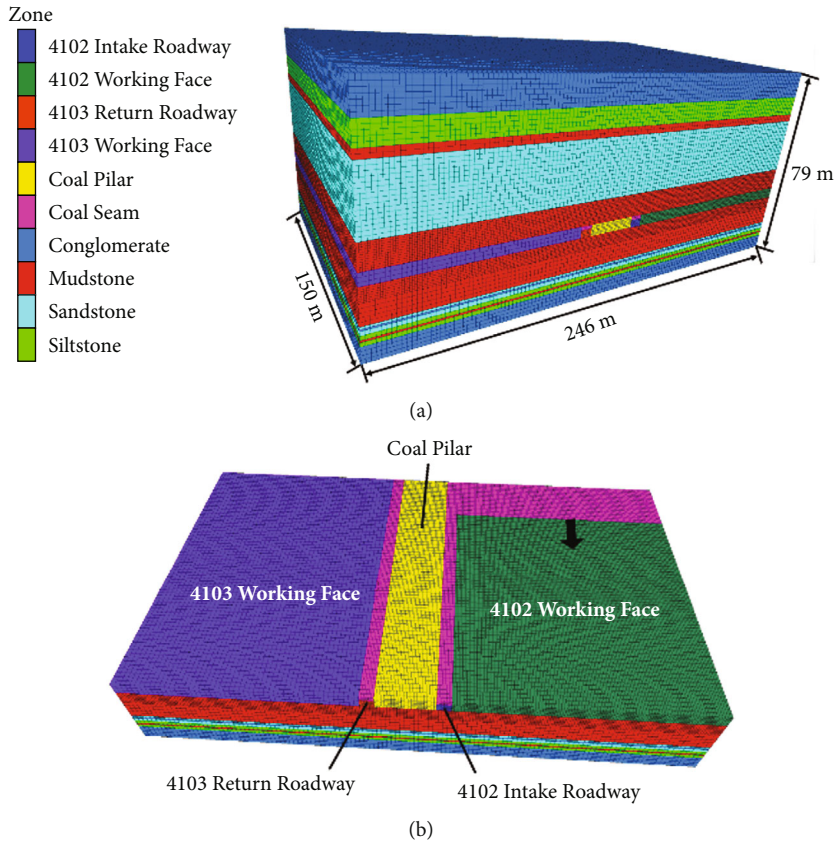

Figure 8: Geometric model of simulations.

The vertical stress in the summary simulation results is shown in Figures 13 and 14.

In Figure 13, during the driving of the 4102 headgate, the vertical stress in the coal pillar caused by the different coal pillar width is different:

(a) When the width of the coal pillar is 15 m and 25 m, the stress in the coal pillar presents a single peak parabolic distribution, and the peak position is not in the center of the coal pillar. In the case of 15 m coal pillar, the peak center is biased to the side of the coal pillar near the roadway, and the deviation distance is about 1.5 m; when the coal pillar widens to 25 m, the vertical stress in the coal pillar gradually presents a trapezoidal distribution, and the peak position shifts from the side of the roadway to the side of the goaf. The deviation distance increases with the increase of the width of the coal pillar, and the deviation distance is about 1.5 m

(b) When the coal pillar width is 33 m and 46 m, the stress distribution in the coal pillar is the same as that before the coal pillar width is not reduced. In these two cases, the peak value is in the form of "a hump with two peaks." When the coal pillar is 33 m, the peak value of the coal pillar is at 16 m and 27 m into the coal pillar, and the peak vertical stress in the range of "hump" is close to the original rock stress which can be considered as an elastic core zone with good bearing capacity; when the coal pillar is 44 m, the peak of the coal pillar is 12 m and 27 m deep into the coal pillar

(c) When the coal pillars are 15 m and 25 m, the peak stress of the coal pillar is greater than that of the coal pillars of 33 m and 46 m, because the coal pillar is in the high stress area and the stress concentration of the coal pillar is higher; the first two of the coal pillars plastic zone are larger, because the first two of the coal pillar plastic zone are larger, the abutment pressure

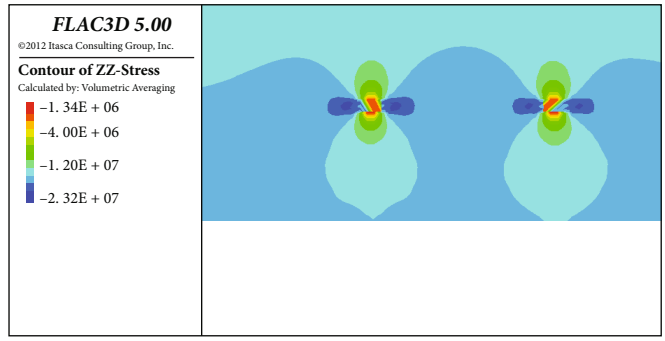

(a) Vertical stress of 0 m advancing the working face

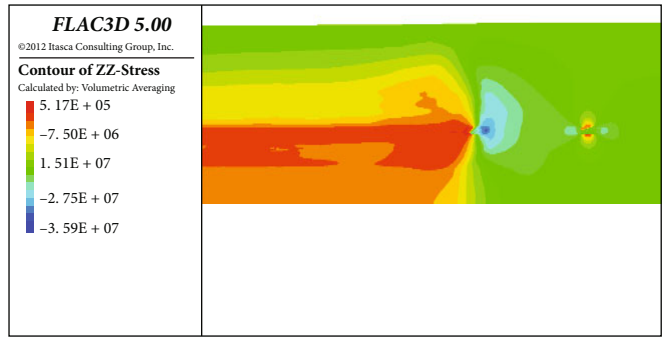

(b) Vertical stress of 40 m advancing the working face

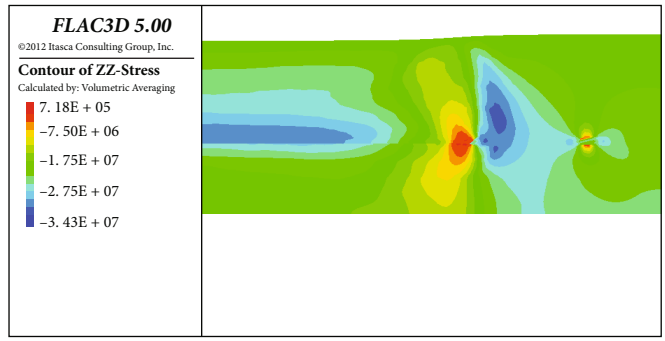

(c) Vertical stress of 80 m advancing the working face

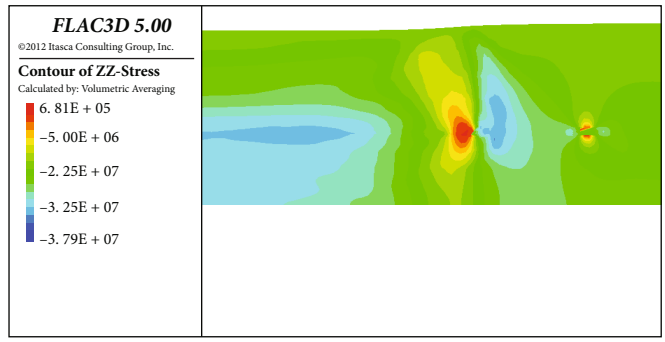

(d) Vertical stress of 120 m advancing the working face

Figure 9: Vertical stress diagram of coal pillar during No. 4102 working face mining.

shifts to the deep part of the coal seam, and the coal at the side edge of the goaf is more fragmented

In Figure 14, during the mining of the 4102 working face, the vertical stress in the coal pillar caused by the different coal pillar width is different:

(a) Compared with roadway driving, the vertical stress in the coal pillar is more concentrated during the mining. The most concentrated stress is when the coal pillar width is 25 m. At this time, the peak stress reaches 38.8 MPa, which is 2.4 times the original rock stress; during the mining period, the vertical

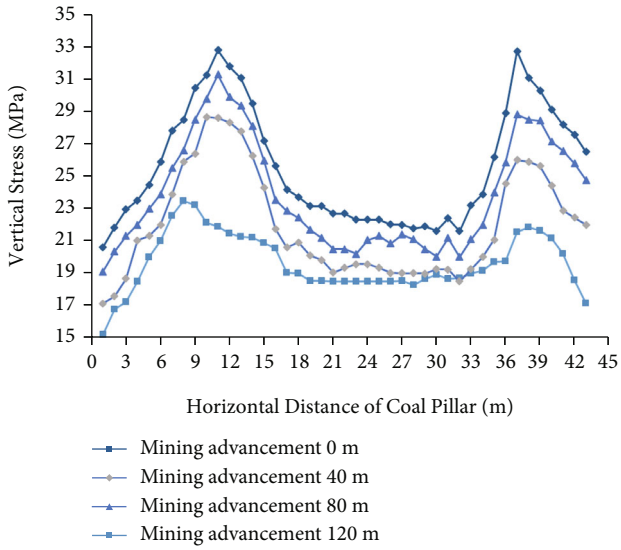

Figure 10: Vertical stress distribution curve of coal pillar during 4102 working face advancing.

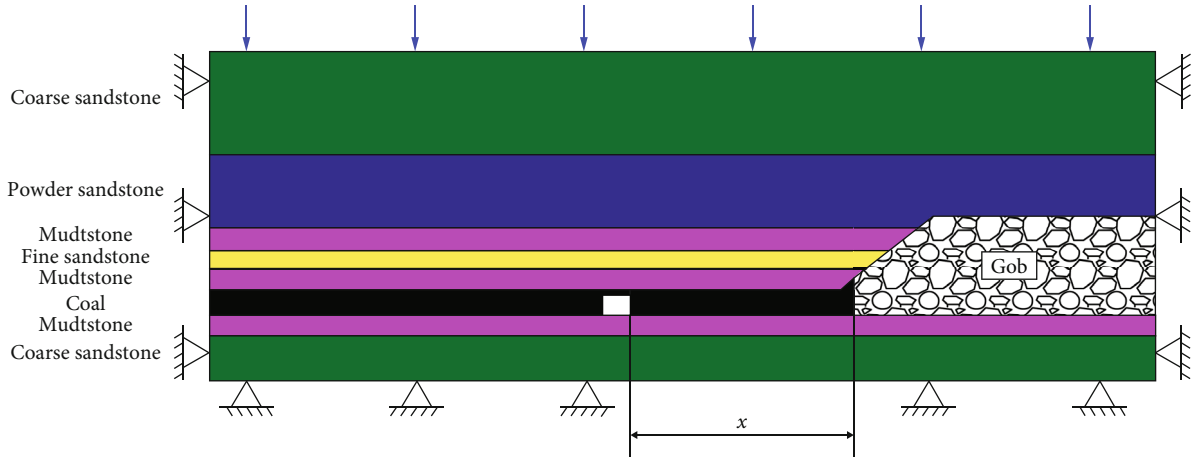

Figure 11: Diagrams of simulation schemes for different coal pillars.

stress curves of the four coal pillars did not change much, and the shape of the stress curves was still similar to that during driving

(b) During the mining period, the low-stress area at the edge of the coal pillar expands, and the peak vertical stress in the coal pillar moves to the inside of the coal pillar. As the coal pillars are subjected to relatively large loads during the mining process, the edges of the coal pillars undergo plastic failure

It can be seen from the above analysis that under the same mining conditions, the smaller the width of the coal pillar, the more concentrated the load on the coal pillar, the peak stress will shift inward, the elastic core range in the middle part will decrease, and the width of the plastic zone will increase. Therefore, discussing the reasonable width of the coal pillar, it should be consider the impact of the stress environment in which the coal pillars are located.

5.4. Comparison of Plastic Zone in the Different Coal Pillars. The range of the plastic zone of coal pillars with different widths is shown in Figure 15.

It can be seen from Figure 16 that when the width of the coal pillar is 46 m and 33 m, a large range of elastic areas can be seen in the coal pillar, there is basically no plastic failure in the elastic area, it has a higher bearing capacity, and the elastic areas of the coal pillar are, respectively, 60% and 55%; when the coal pillar width is 15 m and 25 m, the elastic area in the coal pillar basically disappears, the entire coal pillar has basically undergone plastic failure, the elastic area is basically completely lost, and the proportion of the plastic area is close to 100%. In particular, the 15 m coal pillar has basically lost its bearing capacity due to excessive deformation, and the reason is that the roof has broken at the edge of the goaf. Coupled with the influence of secondary mining, the roof of roadway continues to bend and sink, and the abutment pressure transfers to the coal pillar. Due to the integrated coal has a greater bearing capacity, the crushing

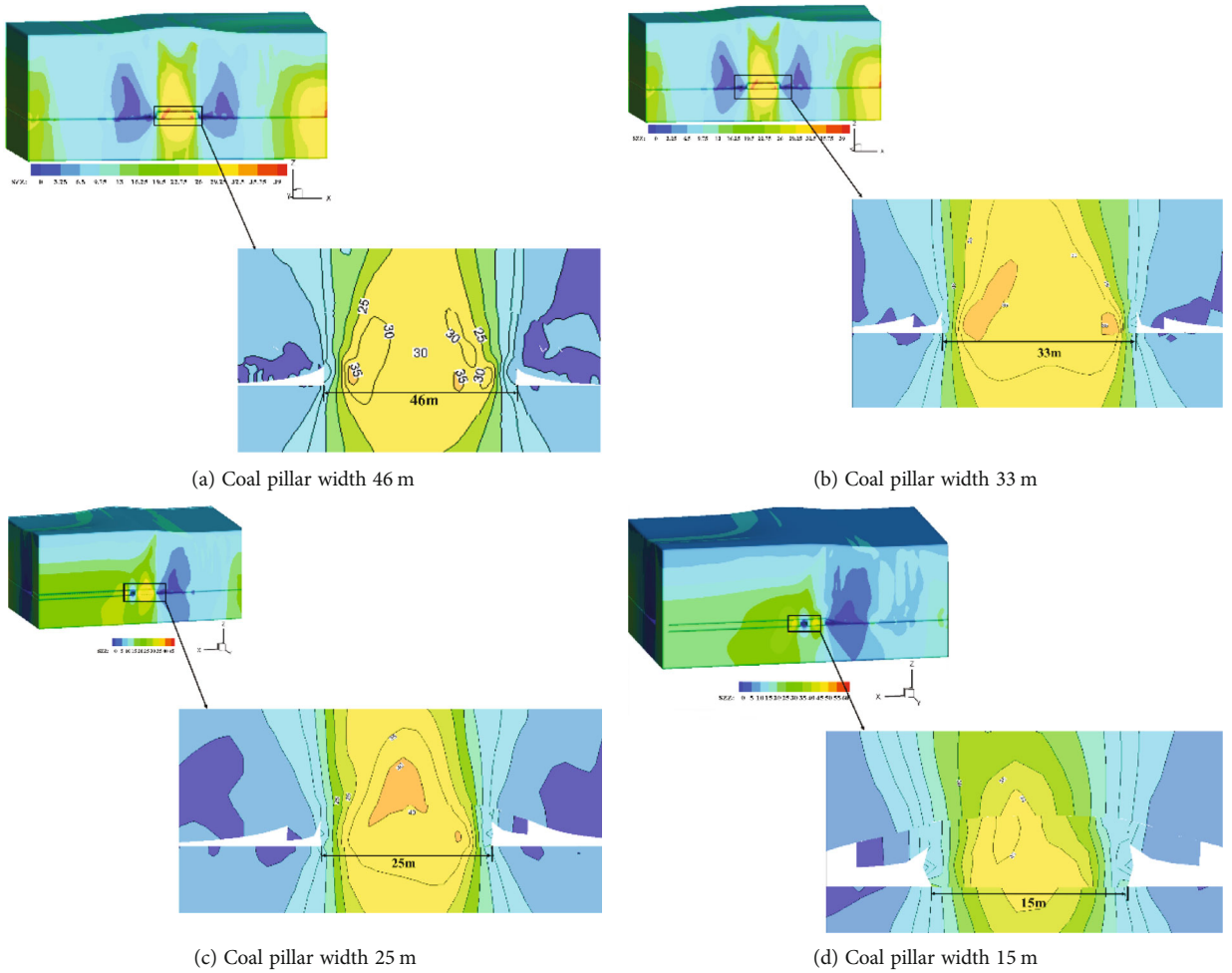

(a) Coal pillar width 46 m

(b) Coal pillar width 33 m

(c) Coal pillar width 25 m

(d) Coal pillar width 15 m

Figure 12: Vertical stress in the different coal pillars width.

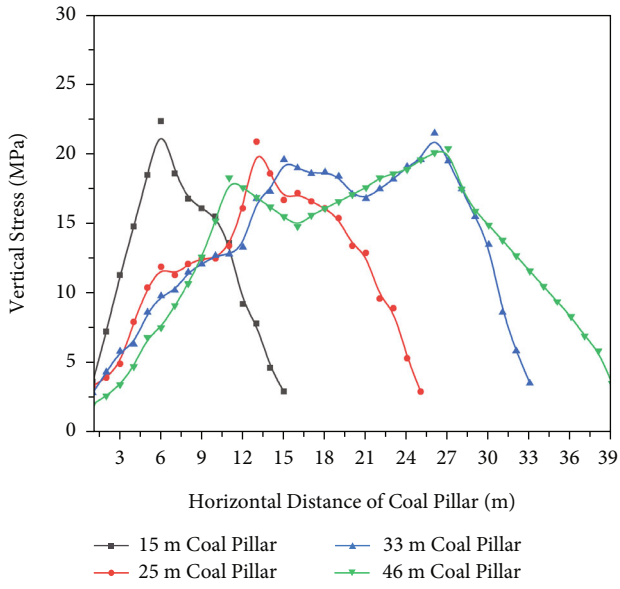

Figure 13: Vertical stress during different pillar driving.

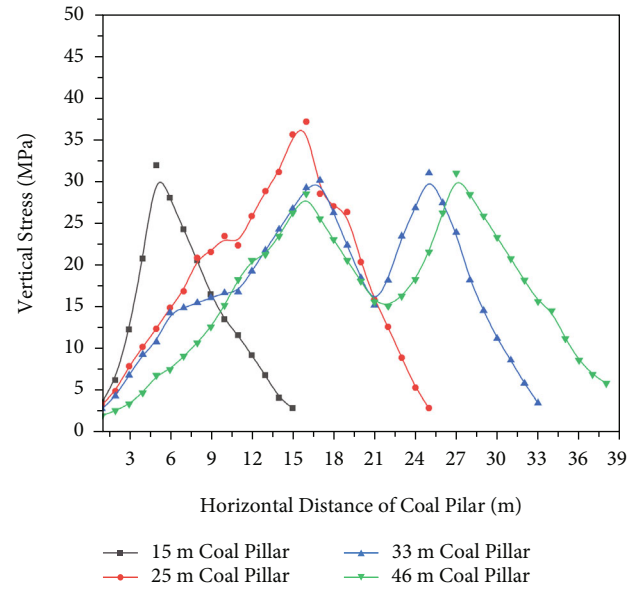

Figure 14: Vertical stress during different pillar mining.

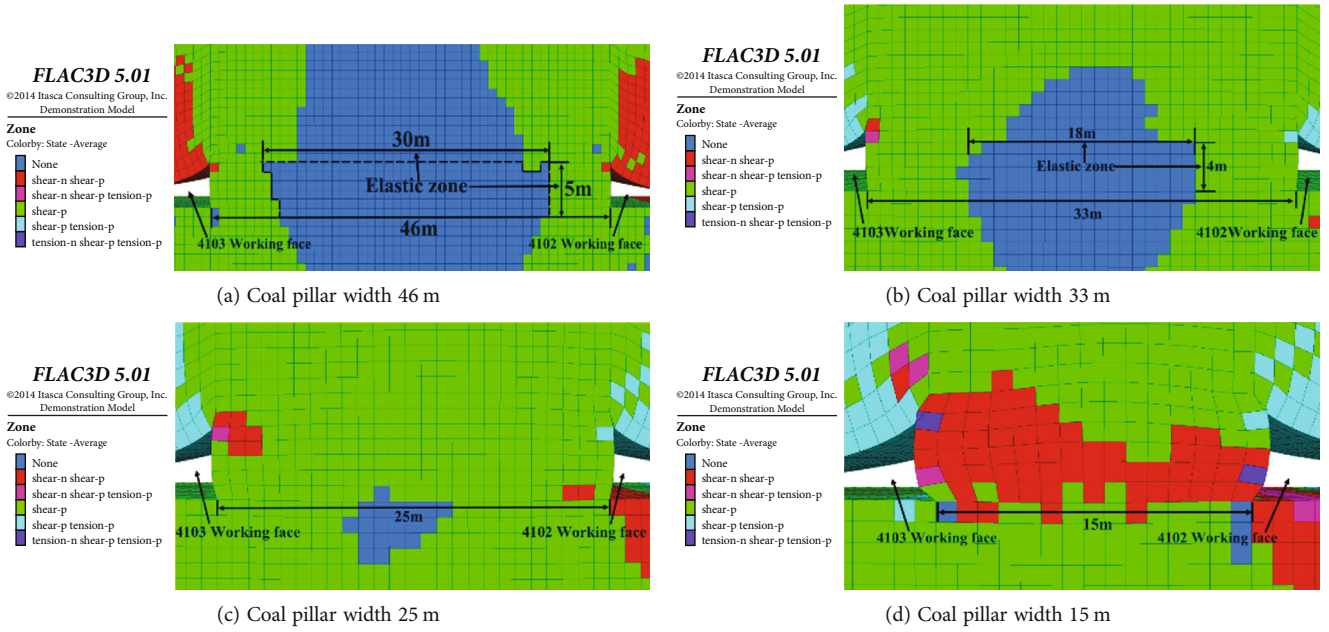

(a) Coal pillar width 46 m

(b) Coal pillar width 33 m

(c) Coal pillar width 25 m

(d) Coal pillar width 15 m

Figure 15: The plastic zones in coal pillars with different widths.

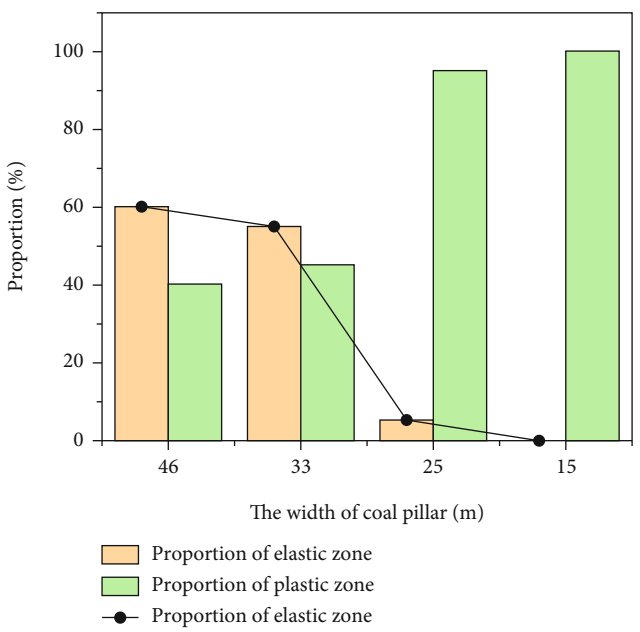

Figure 16: Variation curve of plastic zone in coal pillars with different widths.

scope and impact in surrounding rock of the roadway are smaller than the goaf side. The coal pillar sill will produce a certain range of plastic zone, the bolts located in the broken zone will fail, the bolt supporting capacity will decrease, the degree of broken roadway surrounding rock will increase, and the stability of coal pillar will decrease.

5.5. Determination of the Width of the Coal Pillar. In summary, when the coal pillar is 33 m, the vertical stress distribution still presents a form of "a hump with two peaks" during working face mining. The positions of the double peaks are about 18 m and 27 m in the coal pillar, respectively. The range of the "hump" in the coal pillar is roughly 10 m ~12 m. Within this width, the supporting pressure of the coal pillar is at a relatively high level with the superimposed disturbances of the two stopings. Compared with the 46 m coal pillar, the stress level is not significantly increased, and the stress peak change is small. It can be regarded as a certain amount of the coal pillar. The width of the elastic zone has a strong bearing capacity; the coal in other areas of the coal pillar has completely plastically yielded and only has a certain bearing capacity.

Compared with the 33 m coal pillar, the 15 m and 25 m coal pillars have larger plastic zones and higher stress concentration. Although the stress level and the development degree of the plastic zone for the 46 m coal pillars are almost the same as those of the 33 m coal pillars, it is due to the resource utilization, and the width of coal pillar was determined to be 33 m.

6. Field Test

Based on the previous research results, field test of coal pillar retention was carried out on the 4106 headgate in the same panel. The width of section pillar is 33 m, and there are a monitoring section every 100 m to monitor the deformation of the surrounding rock of the roadway during the workface mining (see Figure 17).

During the mining process of the roadway surrounding rock (see Figure 17), the monitoring section is outside the range of 70 m from the working face, and the roadway roof-floor displacement and deformation rate are small, closed to 0 mm/d; in the range of 50 m, the roof subsidence and the deformation of the coal rib convergence have increased to varying degrees. Especially, in the 24 m mining area, the surface displacement in the roadway began to increase rapidly. During the entire mining

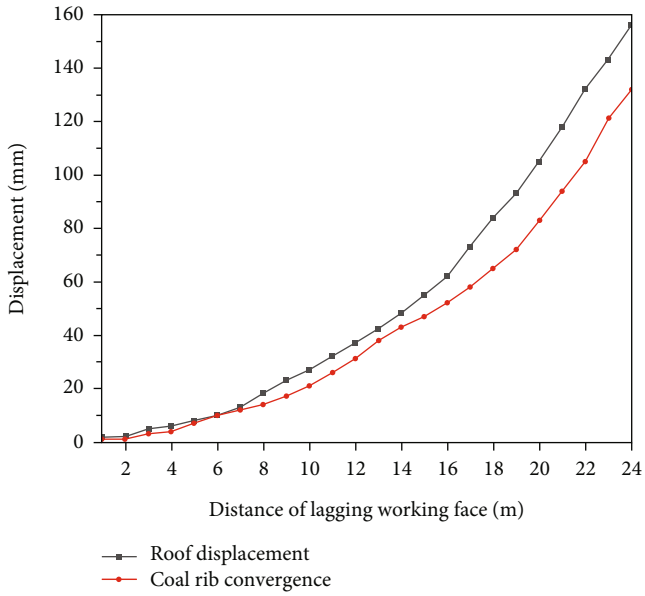

Figure 17: Deformation of surrounding rock of roadway.

Figure 18: Roadway surrounding rock control effect.

process, the maximum roof subsidence was 153 mm, and the maximum displacement of the coal rib convergence was 132 mm. The deformation rate was smaller in the early stage and increased in the later stage. There was no obvious displacement, which proved that the roadway control was reasonable and effective.

The on-site monitoring results show that it is reasonable to leave the coal pillar width of 33 m, and the control effect of the surrounding rock of the roadway is good (see Figure 18).

7. Conclusions

(1) It can be seen from the measured data that the abutment pressure in the coal pillar increasing with the working face mining and presents a form of "a hump with two peaks." The positions of the double peaks are 12 m and 36 m in the coal pillar, and the distances of "two peaks" are 24 m. The peaks are 38.9 MPa and 33.6 MPa, respectively. The range of the curve "hump" is roughly 17 m ~34 m. In the range of 17 m width, the abutment pressure in the coal pillar is between 15 MPa and 20 MPa, which is the original rock stress with little change. It can be regarded as an elastic zone with a certain width in the coal pillar and has a strong bearing capacity; numerical simulation analysis results in a law similar to the measured data ("a hump with two peaks"). Therefore, the coal pillar can be appropriately reduced

(2) The stress concentration in the coal pillar (15 m and 25 m) is 15% ~30% higher than wider coal pillar (33 m and 46 m); the damage area of the plastic zone also accounts for a larger proportion. The ratio is 45% and 46%, and there is still a large area of elastic zone; the coal pillars are basically completely damaged when the coal pillars width is 25 m and 15 m, and the plastic zone accounts for 100%. Based on comprehensive considerations, the width of the remaining coal pillars is determined to be 33 m

(3) After field measurement, it is found that the maximum displacement of the roof and floor is 153 mm, the maximum displacement of the two sides is 132 mm, and the deformation is small; the deformation rate is small in the early stage and increased in the later stage. There is no obvious displacement changed, which proves that the roadway control is reasonable. The overall displacement during the mining period is not large, which proves that the coal pillar has a good field application effect and can be used under the same geological conditions

Data Availability

The data used to support the findings of this study are included within the article. The excel data used to support the findings of this study are included within the supplementary information file.

Conflicts of Interest

The authors declare that they have no conflicts of interest.

Acknowledgments

This work was financially supported by the National Natural Science Foundation of China (No. 52174138) and Graduate Innovation Project of Jiangsu Province (KYCX21_2366).

References

[1] X. H. Li, M. H. Ju, S. K. Jia, and Z. Chong, "Study of influential factors on the stability of narrow coal pillar in gob-side entry driving and its engineering application," *Journal of Mining & Safety Engineering*, vol. 33, no. 5, pp. 761–769, 2014.

[2] W. R. He, F. L. He, D. D. Chen, and Q. Chen, "Pillar width and surrounding rock control of gob-side roadway with mechanical caved mining in extra-thick coal seams under hard-thick main roof," *Journal of Mining & Safety Engineering*, vol. 37, no. 2, pp. 349–358, 2020.

[3] L. G. Wang and X. X. Miao, "Study on catastrophe characteristics of the destabilization of coal pillars," *Journal of China Coal Society*, vol. 36, no. 1, pp. 7–11, 2007.

[4] Z. Yuan, Z. Wan, F. Li, and C. Hou, "Stability of coal pillar in gob-side entry driving under unstable overlying strata and its coupling support control technique," *International Journal of Mining Science and Technology*, vol. 23, no. 2, pp. 204–210, 2013.

[5] D. Ma, J. J. Wang, X. Cai et al., "Effects of height/diameter ratio on failure and damage properties of granite under coupled bending and splitting deformation," *Engineering Fracture Mechanics*, vol. 220, article 106640, 2019.

[6] R. Guy, M. Kent, and F. Russell, "An assessment of coal pillar system stability criteria based on a mechanistic evaluation of the interaction between coal pillars and the overburden," *International Journal of Mining Science and Technology*, vol. 27, no. 1, pp. 9–15, 2017.

[7] G. F. Songa and S. L. Yang, "Probability and reliability analysis of pillar stability in South Africa," *International Journal of Mining Science and Technology*, vol. 28, no. 4, pp. 715–719, 2018.

[8] R. Mohammad, F. H. Mohammad, and M. Abbas, "Development of a time-dependent energy model to calculate the mining-induced stress over gates and pillars," *Journal of Rock Mechanics and Geotechnical Engineering*, vol. 7, no. 3, pp. 306–317, 2015.

[9] Q. Sun, J. Zhang, F. Ju, L. Li, and X. Zhao, "Research and application of schemes for constructing concrete pillars in large section finishing cut in backfill coal mining," *International Journal of Mining Science and Technology*, vol. 25, no. 6, pp. 915–920, 2015.

[10] L. J. Ding and Y. H. Liu, "Stress distribution and failure depth analysis of mining floor in close distance thick coal seam group," *Fresenius Environment bulletin*, vol. 27, no. 3, pp. 1896–1903, 2018.

[11] L. X. Wu and J. Z. Wang, "Calculation of width of yielding zone of coal pillar and analysis of influencing factors," *Journal of China Coal Society*, vol. 20, no. 6, pp. 625–631, 1995.

[12] X. G. Zheng, Z. G. Yao, and N. Zhang, "Stress distribution of coal pillar with gob-side entry driving in the process of excavation & mining," *Journal of Min-ing & Safety Engineering*, vol. 29, no. 4, pp. 459–465, 2012.

[13] C. Q. Han, K. Z. Zhang, and X. B. Xu, "Study on failure regularity and reasonable dimension of district sublevel small coal pillar," *Journal of Mining & Safety Engineering*, vol. 24, no. 3, pp. 370–373, 2017.

[14] J. B. Bai, C. J. Hou, and H. F. Huang, "Numerical simulation study on stability of narrow coal pillar of roadway driving along goaf roadway," *Chinese Journal of Rock Mechanics and Engineering*, vol. 23, no. 20, pp. 3475–3479, 2004.

[15] H. P. Kang, D. L. Niu, and Z. Zhang, "Deformation characteristics of surrounding rock and supporting technology of gob-side entry retaining in deep coal mine," *Chinese Journal of Rock Me-chanics and Engineering*, vol. 29, no. 10, pp. 1977–1987, 2010.

[16] K. X. Zhang, Y. D. Jiang Yaodong, and Z. B. Zhang, "Determining the reasonable width of narrow pillar of roadway in gob entry driving in the large pillar," *Journal of Mining & Safety Engineering*, vol. 31, no. 2, pp. 255–262, 2014.

[17] C. J. Hou and X. J. Li, "Stability principle of large and small structure of surrounding rock in fully mechanized caving roadway along goaf," *Journal of China Coal Society*, vol. 26, no. 1, pp. 1–6, 2001.

[18] H. P. Kang, L. X. Yan, and X. P. Guo, "Multi-lane retaining wall rock is arranged in the mining face. Deformation characteristics and support technology," *Chinese Journal of Rock Mechanics and Engineering*, vol. 31, no. 10, pp. 2022–2036, 2013.

[19] H. P. Kang, X. Zhang, L. P. Si, Y. Wu, and F. Gao, "In-situ stress measurements and stress distribution characteristics in underground coal mines in China," *Engineering Geology*, vol. 116, no. 3, pp. 333–345, 2010.

[20] H. P. Kang, "The development of roadway surrounding rock control technology in China for 70 years and its prospect," *Chinese Journal of Rock Mechanics and Engineering*, vol. 46, no. 1, pp. 1–30, 2021.

[21] N. Zhang, F. Xue, and C. L. Han, "Technical challenges and countermeasures of the co-excavation of coal and gas with no-pillar retains in deep coalmine," *Journal of China Coal Society*, vol. 40, no. 10, pp. 2251–2259, 2015.

[22] Y. P. Wu, H. W. Wang, and P. S. Xie, "Analysis of surrounding rock macro stress arch-shell of longwall face in steeply dipping seam mining," *Journal of China Coal Society*, vol. 37, no. 4, pp. 559–564, 2011.

[23] D. Ma, J. X. Zhang, H. Y. Duan et al., "Reutilization of gangue wastes in underground backfilling mining: overburden aquifer protection," *Chemosphere*, vol. 264, article 128400, 2021.

[24] M. C. He, F. Zhao, and M. Ca, "A novel experimental technique to simulate pillar burst in laboratory," *Rock Mechanics and Rock Engineering*, vol. 48, no. 5, pp. 1833–1848, 2015.

[25] D. S. Li, D. H. Li, and C. S. Song, "Modified application of limit equilibrium theory in strip coal pillar design," *Journal of Liaoning Technical University*, vol. 1, no. 1, pp. 125–128, 2003.

[26] G. S. Jia and L. J. Kang, "Study on the stability of coal pillars in mining roadways for fully mechanized caving mining," *Journal of China Coal Society*, vol. 27, no. 1, pp. 7–10, 2002.

[27] Y. F. Zou and H. B. Chai, "Research status and existing problems of stability of strip coal pillars in China," *Journal of Mining and Safety Engineering*, vol. 2, no. 1, pp. 78–83, 2006.

[28] H. X. Zhou, Q. L. Yang, and Y. P. Cheng, "Methanedrainage and utilization in coal mines with strong coal and gas outburst dangers: a case study in Luling mine, China," *Journal of Natural Gas Science and Engineering*, vol. 20, no. 6, pp. 357–365, 2014.

[29] S. L. Kong, Y. P. Cheng, and T. X. Ren, "A sequential approach to control gas for the extraction of multi-gassy coal seams from traditional gas well drainage to mining-induced stress relief," *Applied Energy*, vol. 131, no. 23, pp. 67–78, 2014.

[30] W. Shi, H. T. Liu, C. Liang, and H. S. Jia, "Research on mine pressure behave law in mining of face under the coal pillar," *Advanced Materials Research*, vol. 217, no. 43, pp. 1721–1724, 2011.

[31] J. X. Yang and C. Y. Liu, "Calculation and analysis of stress in strata under gob pillars," *Journal of Central South University*, vol. 22, no. 3, pp. 1026–1036, 2015.

[32] J. X. Yang and C. Y. Liu, "Effects of load distribution exerting on coal pillars on the stress and energy distribution of the floor strata," *Acta Montanistica Slovaca*, vol. 21, no. 2, pp. 102–112, 2016.

[33] D. Ma, S. B. Kong, Z. H. Li, Q. Zhang, Z. H. Wang, and Z. L. Zhou, "Effect of wetting-drying cycle on hydraulic and

mechanical properties of cemented paste backfill of the recycled solid wastes," *Chemosphere*, vol. 282, article 131163, 2021.

[34] D. Broek, *Elementary Engineering Fracture Mechanics*, Springer Science & Business Media, 2012.

[35] D. C. Wang, S. C. Li, and Q. Wang, "Reasonable width of roadway pillar in deep thick coal seam with fully mechanized caving along goaf," *Chinese Journal of Rock Mechanics and Engineering*, vol. 33, no. 3, pp. 539–548, 2014.

[36] X. S. Zhang, "Determination of reasonable width of coal pillar supporting roadway in deep coal seam group along goaf," *Coal Carbon Journal*, vol. 4, no. 1, pp. 28–35, 2011.

[37] H. S. Wang, D. S. Zhang, S. G. Li, W. A. N. G. Lin, and W. U. Lin-zi, "Rational width of narrow coal pillar based on the fracture line location of key rock B in main roof," *Journal of Mining & Safety Engineering*, vol. 31, no. 11, pp. 10–16, 2014.